ACS APPLIED MATERIALS & INTERFACES

LETTER

www.acsami.org

In situ Electrochemical Monitoring of Selective Etching in Ordered Mesoporous Block-Copolymer Templates

Edward J. W. Crossland,[*,†,‡] Pedro Cunha,[§] Sabine Ludwigs,[†,#,⊥] Marc A. Hillmyer,[||] and Ullrich Steiner[*,§,†]

[†]Freiburg Institute for Advanced Studies (FRIAS), University of Freiburg, 79104 Freiburg, Germany

[§]Cavendish Laboratory, J. J. Thomson Avenue, University of Cambridge, Cambridge CB3 0HE, United Kingdom

[#]Freiburg Materials Research Center (FMF), University of Freiburg, Stefan-Meier-Strasse 21, 79104 Freiburg, Germany

[||]Department of Chemistry, University of Minnesota, Minneapolis, Minnesota, 55455, United States

Supporting Information

ABSTRACT: We present a simple in situ electrochemical probe for the selective etching of the PLA component of thin film poly(4-fluorostyrene)-*b*-poly(D,L-lactide) (PFS-*b*-PLA) mesoporous block copolymer templates with a range of highly ordered microphase morphologies. Etching rates between 0.6 and 0.9 nm s^{-1} were measured in electric-field aligned standing PLA cylinders 12 nm wide and up to 800 nm long. The etching rate within a bicontinuous gyroid network morphology is comparable to that of the hexagonally ordered cylindrical array. A microphase-separated, nonaligned but film-spanning PLA pore structure is found in cylinder forming PFS-*b*-PLA films immediately after spin coating that could have applications in patterning of functional nanostructured arrays. Cross-film percolation of the PLA phase is confirmed electrochemically, with an etching rate approximately half that of the highly ordered morphologies. The etching rate is independent of template thickness in all three morphologies.

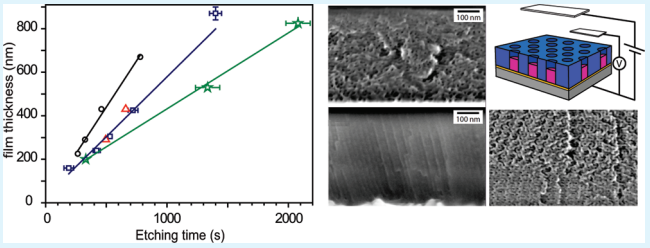

KEYWORDS: block copolymers, thin films, self-assembly, porous materials, nanostructured materials

INTRODUCTION

Membrane-based electrochemical synthesis is an extremely promising approach to the economical fabrication of nanostructured materials.[1] This approach enables the transfer of controlled structural ordering of self-assembling systems into a vast range of functional materials which are synthesized directly in the pores of a preformed template. Electrochemical filling of the pores is possible over large areas with complex (and high aspect ratio) geometries, a regime not readily accessible using top down lithography. Typical mesoporous materials successfully employed in this role include anodized aluminum oxide (AAO),[2] polystyrene colloidal crystals,[3] track-etched polycarbonate membranes,[4] surfactant structured mesoporous silica,[5] and block copolymer films.[6,7] Nanostructured metals, inorganic semiconductors, and semiconducting polymers have all been grown in this manner.

Block copolymers are a particularly interesting templating material due to their wealth of self-assembled, 10 nm scale phase morphologies in a system amenable to solution processing techniques[8−11] A thin film (typically around 1 μm or less) of the phase separated copolymer is subjected to selective degradation of one phase, leaving a porous matrix of the remaining polymer. Copolymers of poly(lactic acid) (PLA) are an attractive alternative to the extensively studied poly(styrene)-*b*-poly(methylmethacrylate) PS-*b*-PMMA system since PLA is susceptible to 'mild' chemical etching by hydrolysis in dilute acid or base.[7,12−14] Copolymers of functional materials (such as conjugated semiconducting polymers) that are easily damaged by aggressive processing steps such as UV exposure (an etch for PMMA) can therefore be patterned directly via self-assembly.[14−16]

The successful application of a porous block copolymer film as a mesoscale template depends on (1) selective etching of one phase and (2) the presence of a fully film-spanning, continuous pore structure with access to the underlying substrate. Asymmetric substrate−polymer interactions in thin films favor alignment of cylinders or lamellae parallel to the substrate (forming a nonporous membrane). Various processing methods have been developed to induce film-spanning ordered microstructures from these microphases such as control of surface interactions, patterning, exposure to a solvent atmosphere, zone casting or annealing, and application of an external electric field in the melt.[17]

A number of ex situ spectroscopic techniques provide suitable probes for selective removal of one block copolymer phase, whereas complete knowledge of the nature and alignment of BCP morphology relies on a combination of direct imaging (cross sectional electron microscopy, atomic force microscopy (AFM)) and scattering techniques. We describe here how a simple in situ electrochemical measurement can be used to measure the selective etching of a PLA copolymer component and act as a probe

Received: January 14, 2011
Accepted: April 14, 2011
Published: April 14, 2011

for film-spanning porosity in a range of poly(4-fluorostyrene)-*b*-poly(D,L-lactide) (PFS-*b*-PLA) morphologies.

The copolymer film is first coated on a conducting substrate and immersed in an etching solution for the PLA phase. By applying a fixed potential to the substrate and measuring the electrochemical current flow with a platinum counter electrode we probe in situ the access of the electrolyte to the underlying substrate through the pore structure. Etching of PLA domains begins from the exposed film surface and proceeds down toward the substrate. While the PLA remains intact it is an effective insulating layer in the cell and the electrochemical current flow is negligible. Complete PLA removal allows contact of the electrolyte with the substrate causing a characteristic onset of current flow through the cell. On the other hand, when the PLA domains do not span the film, the electrolyte remains insulated from the working electrode and no current onset is seen. The solution plays the role of both PLA etchant and a probe electrolyte. The breakthrough time, once calibrated, is also a measure of film thickness.

A full electrochemical characterization of the nature and overall degree of film porosity would require the rigor of electrochemical impedance spectroscopy.[18] Indeed, cyclic voltammetry was recently used to study the removal of PMMA from PS-*b*-PMMA films after etching and provide further details of the pore wall surface chemistry.[19] We do not attempt to achieve such thorough characterization with this method; rather we seek to identify a simple binary indicator of film porosity, and the etching time required. These results are the first example of direct electrochemical measurements made during the copolymer etching procedure itself. The measurement is simple, in situ, and requires no additional equipment, complex analysis or processing steps.

EXPERIMENTAL SECTION

Cylinder forming (M_w = 34 kg mol^{-1}, polydispersity index PDI = 1.14, PLA mass fraction 35%) and gyroid forming (M_w = 37 kg mol^{-1}, PDI = 1.21, PLA mass fraction 40%) PFS-*b*-PLA diblock copolymers were synthesized using a previously published procedure.[7,20]

Silicon substrates coated with 40 nm gold by thermal evaporation were used as the conducting substrates (cleaned before use by sonication in acetone and snow-jet cleaning). Copolymer films with thicknesses up to 800 nm were spin-cast from toluene solutions. These films were dried at 60 °C for 2 h to remove residual solvent and used without further processing. To produce ordered standing arrays of PLA cylinders, films were annealed at 180 °C under nitrogen atmosphere in the presence of a 120 V μm^{-1} DC electric field for 35 h.[7] Gyroid networks were prepared by annealing under the same thermal conditions without the application of an electric field. PLA homopolymer was taken from the precursor polymer used to synthesized the block copolymer. This material had a molecular weight of 10 kg mol^{-1} and a PDI of 1.12.

DC current measurements were made using a CH Instruments potentiostat in a standard three electrode setup. The Au substrate supporting the copolymer film was the working electrode (V_{WE}), a platinum wire acted as counter electrode and a Ag/AgCl (3 M KCl) electrode was the reference. Active areas of 0.07 cm^2 were defined in the cell using kapton masking tape (Dupont). The standard cell electrolyte was a 0.05 M NaOH solution in deionized water containing 40% methanol by volume. Typical open circuit voltages (V_{OC}) were between −100 and −150 meV.

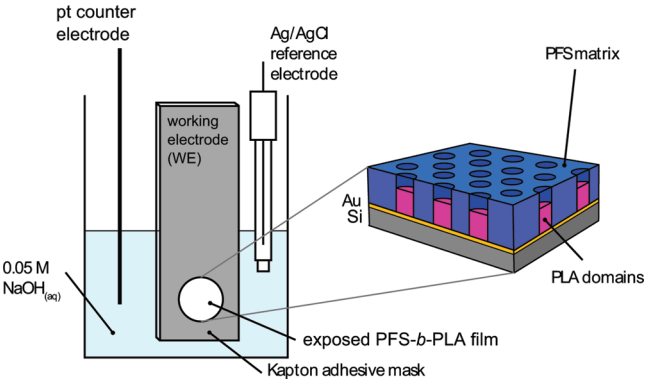

Figure 1. Schematic of a three-electrode cell comprising counter electrode, reference electrode, and Au-coated silicon working electrode coated with the polymer film to be tested. Kapton masking tape ensures that a known area of the film is exposed to the 0.05 M $NaOH_{aq}$ electrolyte solution. A schematic of a vertically aligned cylinder forming PFS-*b*-PLA copolymer film is also included.

Ellipsometry measurements were made using a Nanofilm EP3 spectroscopic ellipsometer with a 532 nm laser. Homopolymer PLA films of ~100 nm were spin coated onto precharacterized Si substrates. Measurements in the dry state (assuming an extinction coefficient of zero) gave a best-fit PLA refractive index of 1.47. In-situ etching measurements were recorded in a liquid cell with a 60° angle of incidence. Ellipsometric data was fitted for the film thickness assuming no change in the refractive index during etching.

Electrochemical deposition of platinum was conducted in a 3-electrode cell at V_{WE} = +0.1 V vs Ag/AgCl in an aqueous solution of 20 mM H_2PtCl_6 containing 20% methanol by volume. Cross-sectional SEM images were made after fracturing the substrate while immersed in liquid nitrogen.

RESULTS AND DISCUSSION

Etching of Homopolymer PLA Films. Figure 1 shows a schematic view of the three-electrode cell used to probe PLA degradation. We look first at a simple system consisting of a 100 nm homopolymer film of PLA (*h*-PLA) on an Au-coated silicon substrate with a 0.05 M $NaOH_{(aq)}$ electrolyte. Figure 2 shows the cathodic (reduction) current at an applied substrate potential of V_{WE} = −50 mV as a function of time, showing a cathodic onset after ~300 s. The thickness of the PLA film determined by in situ ellipsometric fitting of an identical film on a silicon substrate under identical degradation conditions is shown alongside. The current onset corresponds to the complete removal of PLA, corresponding to a breakthrough of the electrolyte to the substrate. After 425 s, the cathodic current peaks before decaying to a steady state anodic current after 650 s (Figure 2b inset). The steady-state current was dependent on V_{OC} (which varied slightly with each batch of Au-coated substrates), but for given V_{OC} increased linearly with methanol concentration (Figure 2b) suggesting that methanol oxidation is the likely source. This is consistent with studies of methanol oxidation at gold surfaces at high pH.[21] Importantly, the first onset of cathodic current reflects the transition from an open circuit to electrolytic contact and was not dependent on V_{WE} (or V_{OC}) over the tested range of −200 to 200 mV. The electrochemical origin of the cathodic transient remains undetermined, however

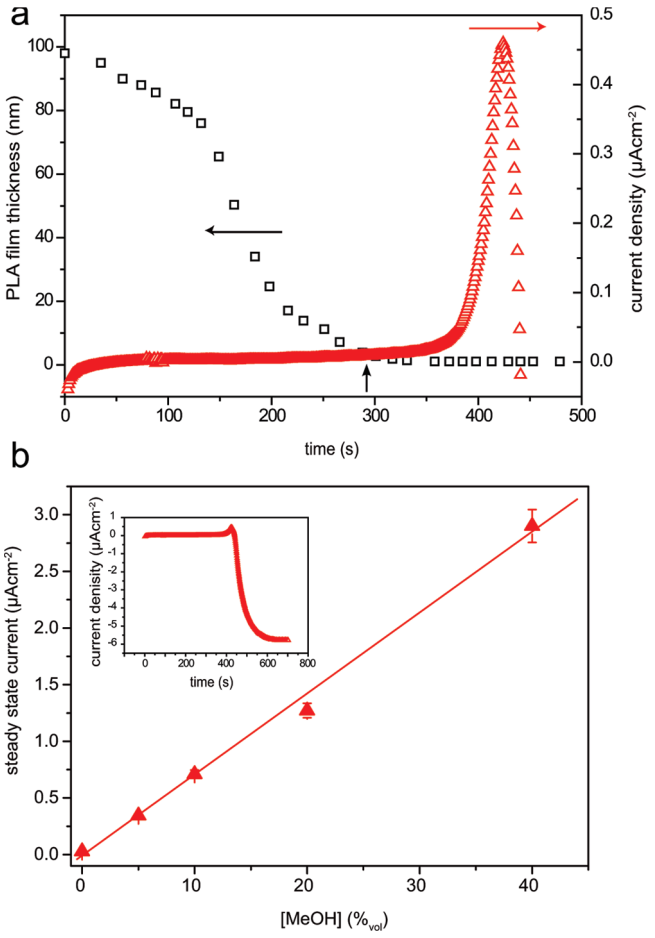

Figure 2. (a) Cathodic current (△) as a function of time for a *h*-PLA film on an Au-coated Silicon substrate alongside the film thickness determined by ellipsometry (□) of an identically prepared film on silicon. The (labeled) onset of cathodic current at ~300 s is determined as the point at which current exceeded 4 times the standard deviation of the background current. A complete view of the current trace is shown in the inset in b. (b) Final steady-state current (anodic) as a function of methanol concentration.

PLA degradation products in the vicinity of the substrate are expected to lower local pH, leading to a transient positive shift in V_{OC}.

Etching of PFS-*b*-PLA Templates. Equivalent electrochemical measurements to those in Figure 2a were made on PFS-*b*-PLA copolymer films on Au-silicon substrates to probe the presence of film-spanning porosity. The range of microphase morphologies, summarized by the cross sectional SEM images and schematics in Figure 3a, were achieved by tailoring the PFS:PLA volume ratio (i.e., molecular synthetic design) and by changes in film processing. A cylinder-forming PFS-*b*-PLA film was annealed at 180 °C (above the glass transition temperature of PFS and PLA blocks) both with and without the application of a vertical, film-spanning electric field in a capacitor geometry. The effect of the electric field is to produce vertical alignment of the cylindrical PLA domains ("standing cylinders") which are otherwise expected to lie parallel to the substrate ("lying cylinders") because of asymmetric polymer−substrate interactions.[7,22] A third microphase morphology was observed in the cylinder-forming copolymer film immediately after spin coating (before any thermal annealing) which we refer to as "as-coated cylinders". Finally, a bicontinuous gyroid morphology (with PLA minority phase) was prepared by thermally annealing a second PFS-*b*-PLA copolymer at 180 °C (described in the Experimental Section and in detail elsewhere).[20,23]

We look first at the thermally annealed cylinder-forming copolymer films. The form of the cell current curve measured through the standing cylinders film (after E-field annealing) was identical to Figure 2 (see the Supporting Information); we therefore attribute the observation of a current onset to the complete etching of PLA minority domains which fully penetrate the film. Measurement of the lying cylinders morphology, on the other hand, showed no onset of current after many hours, indicating that the PLA cylinders are not film-spanning. This conclusion is consistent with the horizontal pores visible in the SEM cross section (Figure 3a) and indicates that the PFS matrix phase is an effective insulator for the electrolyte. Wei et al. also found negligible porosity in CTAB surfactant-templated silica films with a lying cylinder morphology using electrochemical impedance spectroscopy.[24] In contrast to surfactant patterning of silica which involves a high temperature (~400 °C) firing stage and associated material shrinkage we do not expect the opening of smaller pores in the walls separating PLA domains that could lead to continuous porosity even when the primary PLA pores are not film-spanning. Indeed, control experiments showed that even very thin lying cylinder films (<40 nm) showed no measurable current onset in our cell. Measurements of both the gyroid and as-coated cylinder films did show a current onset, proving that the PLA domains run continuously from surface to substrate.

The onset time increased approximately linearly with film thickness in all four studied morphologies (Figure 3b) consistent with an etching front advancing at constant speed (and not diffusion limited) from the exposed film surface through the PLA domains to the substrate. We measured etching rates of between 0.9 and 0.6 nm s^{-1} in 0.05 M NaOH for the standing cylinder morphology (standing cylinders 1 and 2 in Figure 3b). The stated uncertainty reflects the fact that we measured slightly slower etching rates on repeat measurements some 6 months apart in our laboratories after preparation of a fresh batch of NaOH etching solution.[25] When measured consecutively and with the same etching solution (standing cylinders 2, gyroid and as-coated cylinders), the standing cylinder and gyroid morphologies etched at the same rate of 0.6 nm s^{-1} in 0.05 M NaOH while the as-coated cylinder morphology etched at a rate of 0.4 nm s^{-1}. The comparable etching rates of standing cylinders and gyroid morphologies reflect the presence of vertical (or close to vertical) pores running directly from surface to substrate. The slower etching rate of the as-coated cylinders can be explained by the presence of nonvertical, indirect (i.e., longer) tortuous PLA domain pathways through the film.

The morphology of the pore structure in the as-coated cylinder films was further studied by electrochemical deposition of platinum metal into the etched films (20 mM aqueous solution of H_2PtCl_6) followed by final removal of the surrounding PFS template. The electrochemical deposition begins upward from the underlying working electrode and produces a positive replica of the pore structure that is more easily visible in SEM. Replication of the standing cylinders, for example, produces standing arrays of nanowires up to 800 nm in length and ~12 nm in diameter (Figure 3c). Replication of the as-coated cylinder template reveals the internal tangled network structure that is self-supporting after removal of the polymer matrix (Figure 3d). The structure is consistent with a microphase separated yet

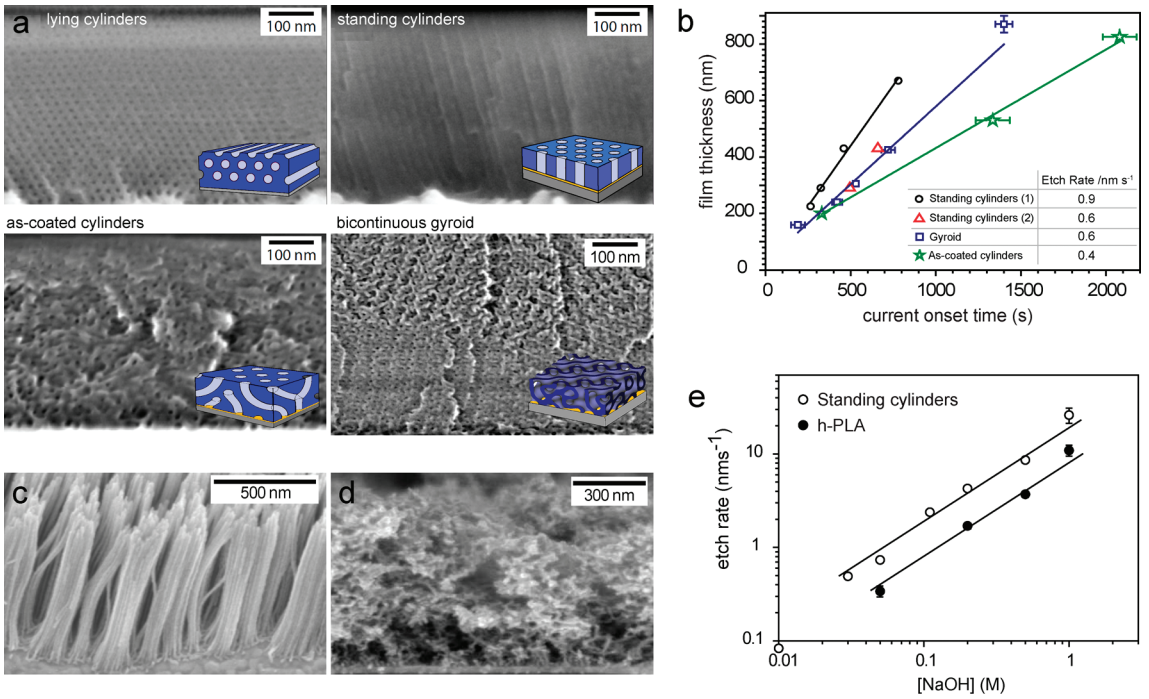

Figure 3. (a) Freeze-fracture cross-sectional SEM images of PFS-*b*-PLA copolymer morphologies after PLA etching (morphologies described in text). (b) Plot of template thickness against current onset time with linear fitting for the morphologies in image a. Etching rates (inset) are extracted from the fitted gradient. Error bars from determination of current onset are smaller than the symbol size when not shown. (c, d) Pt replication of the standing cylinders and as-coated cylinders templates and removal of PFS template by UV ozone exposure. (e) Film etching rate as a function of NaOH concentration for standing PFS-*b*-PLA cylinders (○) and *h*-PLA (•) with first-order linear interpolation. The film thicknesses were 430 nm (standing cylinders) and 415 nm (*h*-PLA).

nonaligned microstructure which we assume is kinetically trapped by the removal of solvent during casting (shown schematically in Figure 3a). We have observed a similar film-spanning morphology after spin coating in a semiconducting triphenylamine side group block copolymer with a sacrificial PLA component that has direct application in patterning of donor−acceptor bulk heterojunction structures.[15]

The etching rate of PLA is pH-dependent, increasing linearly with NaOH concentration in both *h*-PLA and standing cylinder PFS-*b*-PLA films over the studied range (0.03 to 1 M) and reaching rates in excess of 10 nms^{-1} in 1 M etchant solutions (Figure 3e). The etching rate of the standing PLA cylinders was roughly 2.5 times faster than that of the homopolymer films in this concentration range. The observation of faster PLA etching within copolymer domains when compared to the homopolymer is not currently understood. We have considered plausible differences between the BCP and homopolymer PLA environments shown to exist in other copolymer materials (such as differences in stretched chain conformation,[26,27] partial crystallinity[28,29] or the presence of trapped solvent molecules) but can identify no compelling, unambiguous explanation for the difference in rate of PLA hydrolysis.

CONCLUSION

We present a straightforward in situ measurement of the selective degradation of PLA from PFS-*b*-PLA copolymer films with distinct film-spanning porous morphologies on conducting substrates. The PLA etching rate in films exposed to 0.05 M NaOH(aq) solutions was between 0.6 and 0.9 nm s^{-1} for thermally annealed, vertical arrays of cylindrical domains and gyroid networks, approximately twice as fast as for microphase separated but nonaligned films immediately after spin coating without thermal annealing. The etching time is not limited by diffusion through the pore structure in the concentration and thickness range studied. Combined imaging and electrochemical probes prove that a film-spanning pore structure is present in cylinder-forming PFS-*b*-PLA films with no additional processing required beyond spin coating. The removal of time-costly alignment stage is a major advantage from the perspective of large scale porous membrane and templating applications.

ASSOCIATED CONTENT

Supporting Information. Additional figure (PDF). This material is available free of charge via the Internet at http://pubs.acs.org.

AUTHOR INFORMATION

Corresponding Author

*E-mail: e.crossland1@physics.ox.ac.uk (E.J.W.C.); u.steiner@phy.cam.ac.uk (U.S.).

Present Addresses

‡Department of Physics, Clarendon Laboratory, Parks Road, Oxford, OX1 3PU, U.K.

⊥Institute of Polymer Chemistry, University of Stuttgart, Pfaffenwaldring 55, 70569 Stuttgart, Germany.

ACKNOWLEDGMENT

M.A.H. thanks the Leverhulme Trust for support under their Visiting Professorship program and the National Science

Foundation under award DMR-1006370. E.C. and U.S. thank the EPSRC for funding. S.L. acknowledges financial support from a DFG Emmy Noether stipend and a FRIAS junior fellowship.

REFERENCES

(1) Martin, C. R. *Chem. Mater.* **1996**, *8*, 1739–1746.
(2) Li, F.; Zhang, L.; Metzger, R. M. *Chem. Mater.* **1998**, *10*, 2470–2480.
(3) Bartlett, P. N.; Baumberg, J. J.; Birkin, P. R.; M. C. Netti, M. A. G. *Chem. Mater.* **2002**, *14*, 2199–2208.
(4) Lai, M.; Riley, D. J. *Chem. Mater.* **20006**, *18*, 2233–2237.
(5) Urade, V. N.; Wei, T.; Tate, M. P.; Kowalski, J. D.; Hillhouse, H. W. *Chem. Mater.* **2007**, *19*, 768–777.
(6) Thurn-Albrecht, T.; Schotter, J.; Kästle, G.; Emley, N.; Krusin-Elbaum, T. S. L.; Guarini, K.; Black, C. T.; Russell, M. T. T. T. P. *Science* **2000**, *290*, 2126–2129.
(7) Crossland, E. J. W.; Ludwigs, S.; Hillmyer, M. A.; Steiner, U *Soft Matter* **2007**, *3*, 94–98.
(8) Bates, F. S.; Fredrickson, G. H. *Physics Today* **1999**, 32–38.
(9) Hamley, I. W. *Developments in Block Copolymer Science and Technology*; Wiley: New York, 2004.
(10) Olson, D. A.; Chen, L.; Hillmyer, M. A. *Chem. Mater.* **2008**, *20*, 869–890.
(11) Darling, S. B. *Prog. Polym. Sci.* **2007**, *32*, 1152–1204.
(12) Zalusky, A. S.; Olayo-Valles, R; Wolf, J. H.; Hillmyer, M. A. *J. Am. Chem. Soc.* **2002**, *124*, 12761–12773.
(13) Rzayev, J.; Hillmyer, M. A. *J. Am. Chem. Soc.* **2005**, *127*, 13373–13379.
(14) Botiz, I.; Darling, S. B. *Macromolecules* **2009**, *42*, 8211–8217.
(15) Crossland, E. J. W.; Cunha, P.; Scroggins, S.; Moratti, S.; Steiner, O. Y. U.; Hillmyer, M. A.; Ludwigs, S. *ACS Nano* **2010**, *4*, 962–966.
(16) Boudouris, B. W.; Frisbie, C. D.; Hillmyer, M. A. *Macromolecules* **2008**, *41*, 67–75.
(17) Segalman, R. A. *Mater. Sci. Eng., R* **2005**, *48*, 191–226.
(18) Song, H.; Sung, J.; Jung, Y.; Lee, K.; Dai, L.; Kim, M.; Kim, H *J. Electrochem. Soc.* **2001**, *11*, 849–853.
(19) Li, Y.; Maire, H. C.; Ito, T. *Langmuir* **2007**, *23*, 12771–12776.
(20) Crossland, E. J. W.; Kamperman, M.; Nedelcu, M.; Ducati, C.; Wiesner, U; Smilgies, D. M.; Toombes, G. E. S.; S. Ludwigs, M. A. H.; Steiner, U.; Snaith, H. J. *Nano Lett.* **2009**, *9*, 2807–2812.
(21) Zhang, J.; Liu, P.; Ma, H.; Ding, Y. J. *Phys. Chem. C* **2007**, *111*, 10382–10388.
(22) Olayo-Valles, R.; Guo, S.; Lund, M.; Leighton, C.; Hillmyer, M. A. *Macromolcules* **2005**, *38*, 10101–10108.
(23) Crossland, E. J. W.; Ludwigs, S.; Hillmyer, M. A.; Steiner, U. *Soft Matter* **2010**, *6*, 670–676.
(24) Wei, T.; Hillhouse, H. W. *Langmuir* **2007**, *23*, 5689.
(25) This difference might be caused by a change in pore-wetting properties (surface tension) of the aging NaOH solution. To illustrate this effect, electrodeposition into the etched templates was not possible using electrolytes without the addition of methanol (surface tension = 23 mN m^{-1} compared to 78 mN m^{-1} for water) indicating that no penetration of the open pores occurs. Current flow in the cell (signifying electrolyte penetration) begins immediately upon addition of extra methanol.
(26) Bates, F. S.; Fredrickson, G. H. *Annu. Rev. Phys. Chem.* **1990**, *41*, 525–557.
(27) Karst, D.; Yang, Y. *Polymer* **2006**, *47*, 4845–4850.
(28) Bigg, D. M. *Adv. Poly. Technol.* **2005**, *24*, 69–82.
(29) Sun, Y.-S.; Chung, T.-M.; Li, Y.-J.; Ho, R.-M.; Ko, B.-T.; Jeng, U.-S.; Lotz, B. *Macromolecules* **2006**, *39*, 5782–5788.